Available online at www.sciencedirect.com
SCIENCE DIRECT
Journal of Power Sources 157 (2006) 443–447
JOURNAL OF POWER SOURCES
www.elsevier.com/locate/jpowsour

Electrochemical synthesis of new substituted manganese oxides for lithium battery applications

E. Machefaux, A. Verbaere, D. Guyomard *

Laboratoire de Chimie des Solides, Institut des Matériaux Jean Rouxel, CNRS, Université de Nantes, B.P. 32229, 44322 Nantes Cedex 3, France

Accepted 1 July 2005
Available online 6 September 2005

Abstract

New Co- and Al-substituted manganese dioxide materials have been prepared by electrochemical synthesis under hydrothermal conditions. The hollandite (α), pyrolusite (β) and γ structures can be stabilized using different experimental conditions. For each structure, the substitution leads to nanostructured compounds with various morphologies made of nanosized crystals and to much larger surface areas. Some substituted compounds display larger reversible Li insertion capacities than their non-substituted parents compounds.

Keywords: Lithium; Rechargeable battery; Electrochemical synthesis; Co-substituted manganese oxide; Al-substituted manganese oxide; Nanostructured compound

1. Introduction

Manganese oxides compounds have been largely studied for use as positive electrode materials for Li primary and secondary batteries due to the their low cost, environmental merit and easy preparation [1,2]. Nevertheless, the reversible capacity and the cycling stability of these compounds have to be improved [1,2]. Electrochemical–hydrothermal method is a very versatile technique, which has been used in the preparation of various transition metal oxides, phosphonates [3] and vanadates [4]. Using this route, we synthesized a wide variety of manganese dioxides having various structures such as hollandite (α), pyrolusite (β), γ form, and various controlled morphologies [5–9]. Nevertheless, these materials generally deliver too low a capacity, around 170 mAh g^{-1} at *C*/10 rate [9], to be interesting for application. According to the literature, partial substitution of the transition metal in many cobalt and manganese oxides, such as for instance $LiCoO_2$, $LiMn_2O_4$, $LiMnO_2$ and Birnessite-type MnO_2 results in improved electrochemical performance [10–12]. Given these results, the goal of this work is to synthesize new substituted manganese oxide compounds by using the electrochemical–hydrothermal route.

We report here the preparation of new Al- and Co-substituted manganese oxides, and we examine the consequences of the substitution on the physico-chemical, structural and morphological characteristics of the synthesized compounds. Finally, the electrochemical Li insertion behaviour of these new materials is studied by comparison with non-substituted MnO_2 materials.

2. Experimental

The syntheses were performed in a stainless steel autoclave with provision for connecting the working (Au, 3.5 cm × 4 cm), counter (vitreous carbon plates, 3.5 cm × 4 cm) and Ag^+/Ag reference electrodes to a potentiostat (Mac Pile, Claix, France) used in galvanostatic mode with an oxidation current. The synthesis solution was prepared by dissolution of $MnSO_4$ (0.3 M) in distilled water. The substituent cation, Co^{2+} or Al^{3+}, was added to the initial solution as a soluble salt, $CoSO_4$ (0.3 M) or $Al_2(SO_4)_3$ (0.3 M),

* Corresponding author. Tel.: +33 2 40 37 39 12; fax: +33 2 40 37 39 95.
E-mail address: dominique.guyomard@cnrs-imn.fr (D. Guyomard).

0378-7753/$ – see front matter © 2005 Elsevier B.V. All rights reserved.
doi:10.1016/j.jpowsour.2005.07.035

respectively. In some preparations, Li_2SO_4 (3 M) was added to the initial solution to probe the effect of Li^+ on the obtained material. To determine the effect of synthesis conditions on the structure, we have varied the temperature between 80 and 180 °C, and the pH between 0 and 7 for $CoSO_4$-based solutions and between 0 and 3.5 for $Al_2(SO_4)_3$-based solutions. To maintain good homogeneity in composition and structure, the synthesis was stopped when about 600 mg of deposit were obtained. For all syntheses, the faradaic yield was 100%. After the synthesis, the solid was removed from the electrode, rinsed thoroughly with distilled water and dried for 2 h at 75 °C. Before studying electrochemical performance, samples were ground and heated at 250 °C for 16 h to decrease the amount of structural water.

X-ray diffraction (XRD) patterns (Cu Kα radiation) were obtained using a Siemens D5000 Bragg–Brentano (θ–2θ configuration) diffractometer for the 2θ range 10–75°. The amount P_r of pyrolusite defects, and *Mt* of microtwinning defects in the γ-MnO_2 structure were determined using a method developed by our group based on that proposed by Chabre and Pannetier [1,8,13]. Chemical compositions were determined by atomic absorption spectroscopy with inductively coupled plasma (AAS/ICP analysis), by energy dispersive X-ray analysis (EDX) in a scanning electron microscope (SEM) and at the nanocrystal scale for some samples by EDX in a transmission electron microscope (TEM). Thermogravimetric analysis (TGA) was used to determine the water content in our products. The average Mn oxidation state was determined by redox titration according to reference [8]. Measurements of specific surface area were carried out with the Brauner, Emmett and Teller (BET) method using a Micromeritics 2010 apparatus (with N_2 as adsorbing gas). The surface morphology of the deposits was studied using a JEOL JSM 6400F Scanning Electron Microscope (SEM) operating at 7 keV.

Studies of lithium insertion behavior were performed with standard Swagelok cells made of a composite positive electrode (70 wt.% active material, 20 wt.% carbon black, 10 wt.% PVdF binder), a separator soaked in the electrolyte of composition (1 M $LiPF_6$ in 2:1 ethylene carbonate dimethyl carbonate mixture and a lithium metal negative electrode. Electrochemical properties were determined using a MacPile system (Biologic, Claix, France) by cyclic voltammetry (20 mV h^{-1}) in the voltage range 2–4 V versus Li metal electrode.

3. Results and discussion

To detect the presence of the substituent cation and to determine its content y in $Mn_{1-y}A_yO_{2-\delta}$ (with A = Al, Co), EDX analyses were performed systematically. Fig. 1 presents the results of the composition analysis as a function of the solution pH for syntheses performed at 92 °C. At this temperature, all samples had the γ structure as shown below. For compounds synthesized in presence of $CoSO_4$ in the initial solution, it was observed that for very acidic pH (0 or 1), the MnO_2 powders did not contain cobalt. The MnO_2 powders with the β structure did not contain cobalt irrespective of the solution pH. On the contrary, for pH higher or equal to 4, the cobalt content was homogeneous and close to 3% in compounds belonging to the γ structure. Such a content was confirmed with several products by EDX analysis at the nanocrystal scale using a TEM. These Co-substituted compounds are represented as γ-MnO_2(Co). With $Al_2(SO_4)_3$ in the synthesis solution, the aluminium content increased with both pH and temperature, irrespective of the resulting structures. It was homogeneous at the nanocrystal scale for all samples studied. These Al-substituted compounds are represented as MnO_2(Al). The maximum aluminium content detected was around 21% for a solution pH of 3 and a temperature of 113 °C.

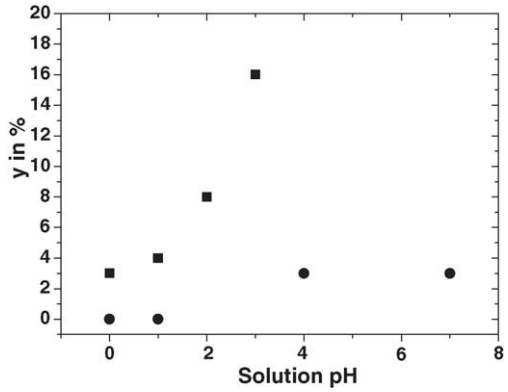

Fig. 1. Evolution of the content of substituent cation y (in %) as a function of the solution pH at 92 °C. Symbols (■ and ●) represent the Al content y in $Mn_{1-y}Al_yO_{2-\delta}$ and the Co content y in $Mn_{1-y}Co_yO_{2-\delta}$, respectively.

Phase diagrams were established from XRD patterns. Pure α-, β- and γ-MnO_2 phases and phase mixtures were obtained according to the experimental conditions employed. All the phases have 1D structures with tunnels running along the *c*-axis. The rutile structure of the pyrolusite phase has tunnels with the size of 1 octahedron edge by 1 octahedron edge (1 × 1). The γ-MnO_2 structure can be seen as a random intergrowth of pyrolusite (1 × 1 tunnels) in the Ramsdellite matrix (1 × 2 tunnels) [14]. This structure contains another type of defects, microtwinning [1]. The Hollandite structure has the most open structure of the series with 2 × 2 open channels [5]. Fig. 2a shows the phase diagram of MnO_2 synthesized from a $MnSO_4/Li_2SO_4$ solution as a function of pH and temperature [6]. The β phase is stabilized at high temperature and high solution pH. Decreasing the temperature and the solution pH leads first to the formation of γ/β mixtures, then to the more open γ structure, and finally to α/γ mixtures. The phase diagram of samples prepared from a $MnSO_4/CoSO_4/Li_2SO_4$ solution is shown in Fig. 2b. The same trends are observed. A decrease in temperature and pH favours the formation of more open structures. However, the temperature range of the β phase at neutral pH decreases because the γ-MnO_2(Co) phase is stable at higher temper-

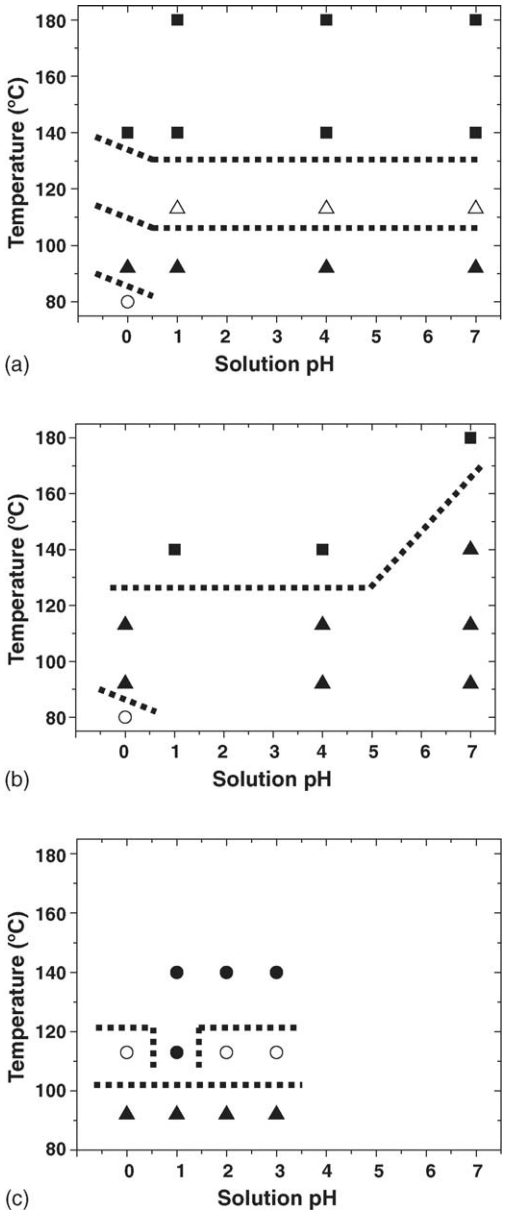

Fig. 2. Phase diagrams in the temperature–pH plane obtained from: (a) $MnSO_4/Li_2SO_4$ solutions, (b) $MnSO_4/CoSO_4/Li_2SO_4$ solutions and (c) $MnSO_4/Al_2(SO_4)_3$ solutions. Symbols (◯, ●, ▲, △ and ■) stand for mixed α/γ phases, the α phase, the γ phase, mixed γ/β phases and the β phase. Note that in (b) only γ phases for pH ≥ 4 are Co-substituted, while all phases in (c) are Al-substituted.

atures, up to 140 °C. Such an increase is more important for pH higher or equal to 4 where Co-substituted samples are stabilized. The phase diagram of Al-substituted MnO_2 synthesized in presence of $MnSO_4/Al_2(SO_4)_3$ is given in Fig. 2c. Surprisingly, no β phase was obtained under the synthesis conditions studied. The XRD patterns of α- and γ-MnO_2(Al) show the absence of any crystallized impurity phase, even at high Al content. We conclude that Al readily enters the α and γ structures. Contrary to compounds prepared in presence of $MnSO_4/Li_2SO_4$ or $MnSO_4/CoSO_4/Li_2SO_4$, the temperature range of the α phase is shifted to higher temperature and higher pH. The formation of the most open structure at higher temperatures could be linked to the presence of some species in the tunnels, which stabilize the α structure. Rietveld refinement of powder XRD data is underway to check this point.

Table 1 summarizes results of some physico-chemical characterizations of MnO_2(Co) and MnO_2(Al) with the γ structure obtained in this study. The average oxidation state of Mn was found to be similar for Co-substituted and non-substituted MnO_2 samples, and ranges from +3.90 to 3.99. XANES experiments performed at the Co K-edge indicated the presence of Co(III) in the γ structure [15]. Results of TGA/DSC analysis revealed that the water content n, for the formulation $Mn_{1-y}A_yO_{2-\delta}\cdot nH_2O$ (A = Co or Al), was between 0.05 and 0.2 and comparable to the water content of non-substituted materials. Under the same experimental conditions, shifting from pure MnO_2 to MnO_2(Co) generally leads to an increase of the surface area by a factor of about two. More spectacularly, shifting from pure MnO_2 and to MnO_2(Al) gives rise to a drastic increase in the surface area by a factor of nearly 10. For example, under given synthesis conditions, pure γ-MnO_2, γ-$Mn_{1-y}Co_yO_{2-\delta}$ and γ-$Mn_{1-y}Al_yO_{2-\delta}$ have surface areas of 17, 26 and 184 $m^2\ g^{-1}$, respectively.

The influence of the substituent cation on the surface morphology of some deposits synthesized under the same conditions is illustrated in Fig. 3. A sharp decrease in the particle size is clearly observed on shifting from MnO_2 to MnO_2(Co) and to MnO_2(Al). This observation is in accordance with the values of the surface area (Table 1). Observations at larger magnification (not shown) indicate variations of the particle morphology with the nature of the substituent cation as well. Large crystals having a size of several tens of nanometers are obtained for Al-substituted compounds.

Fig. 4a and b shows the current versus voltage curves for γ-MnO_2(Co) and γ-MnO_2(Al) having the same content of substituent cation of 3%. These curves show one main

Table 1
Results of physico-chemical characterization of γ-MnO_2(Co) and γ-MnO_2(Al) compounds, compared to non-substituted ones

	γ-MnO_2	γ-MnO_2(Co)	γ-MnO_2(Al)
Water content, n	$0.05 < n < 0.15$	$0.05 < n < 0.20$	$n \approx 0.20$
Surface area ($m^2\ g^{-1}$)	$7 < S_{BET} < 17$	$25 < S_{BET} < 45$	$10 < S_{BET} < 184$
Average oxidation state (Mn)	3.84–3.99	3.90–3.99	–
Formulation	$MnO_{2-\delta}\cdot nH_2O$	$Mn_{1-y}Co_yO_{2-\delta}\cdot nH_2O$	$Mn_{1-y}Al_yO_{2-\delta}\cdot nH_2O$

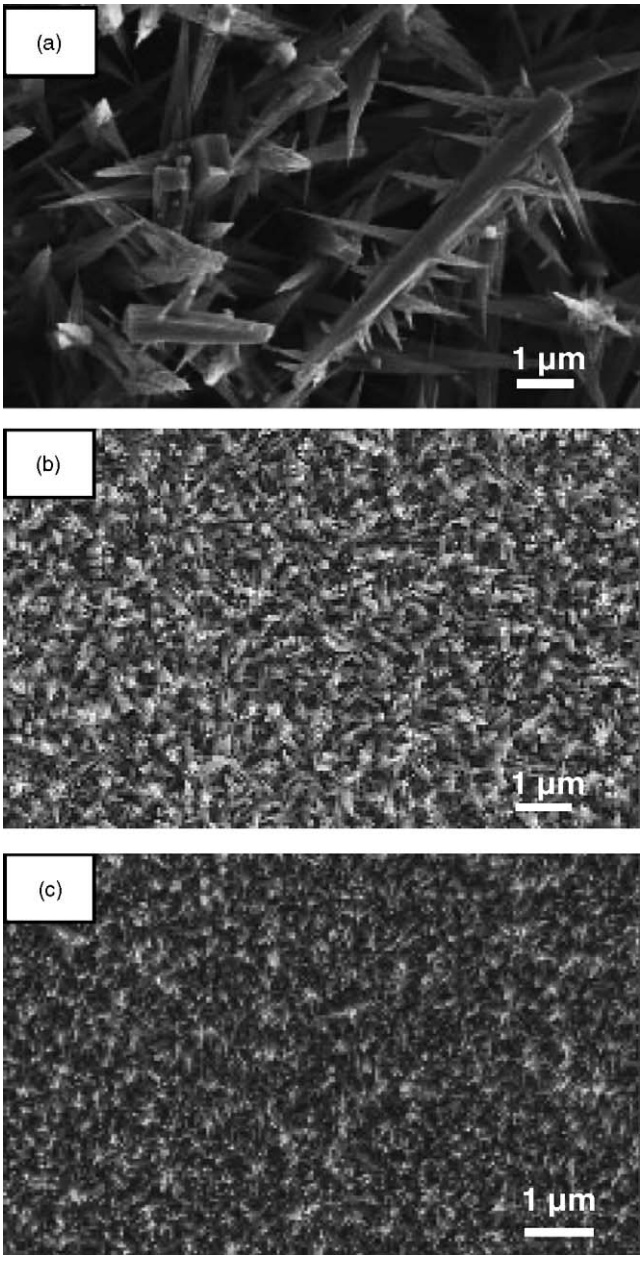

Fig. 3. SEM photographs illustrating the effect of the substituent cation on the surface morphology of samples prepared in the same conditions: (a) non-substituted γ-MnO_2, (b) γ-MnO_2(Co) and (c) γ-MnO_2(Al).

reversible process at about 3 V and one small process in reduction at 3.4 or 3.2 V for MnO_2(Co) or MnO_2(Al), respectively. Such a Li insertion behaviour is typical of Li insertion in the γ-MnO_2 structure [16,17]. As the different processes occur at comparable voltage for γ-MnO_2(Co), γ-MnO_2(Al) and non-substituted γ-MnO_2, it indicates that the presence of the substituent cation does not influence the nature of the Li insertion phenomena.

The amount of Li reversibly inserted within the γ structure can be calculated by integration of these curves (right scale of Fig. 4). Previous results show that it strongly

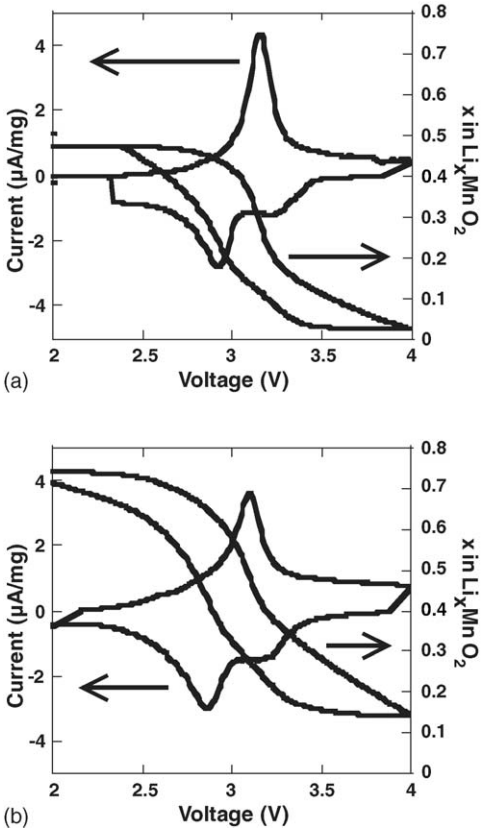

Fig. 4. Current–voltage and Li composition–voltage curves at second discharge-charge cycle for: (a) MnO_2(Co) and (b) MnO_2(Al) with 3% substitution.

depends on the structural parameters of the γ form, i.e. the amount of pyrolusite intergrowth and the amount of microtwinning defects. Thus, to study the influence of the content of substituent cation on the reversible Li uptake, we have compared γ structures of similar P_r and *Mt* rates. The reversible capacity at the second discharge is depicted in Fig. 5 for substituted compounds in comparison with non-substituted γ-MnO_2 with similar structural parameters. It appears that cobalt substitution decreases the reversible capacity, while aluminium substitution increases it.

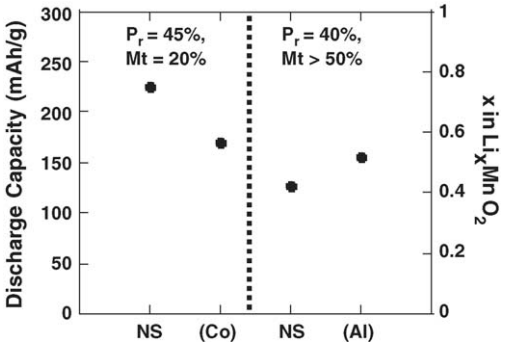

Fig. 5. Reversible Li insertion capacity of substituted γ-MnO_2 compounds compared to non-substituted ones. NS means non-substituted.

4. Conclusions

New Co- and Al-substituted compounds have been synthesized by using the versatile electrochemical–hydrothermal method. It was shown that the substituent cation was readily incorporated in the structure and did not modify the physicochemical characteristics except the surface area which was drastically increased, especially for the Al-substituted compounds. It was observed that the intrinsic electrochemical processes did not depend on the presence or the nature of the substituent cation. Furthermore, aluminium substitution is beneficial to the reversible Li insertion capacity as opposed to cobalt substitution.

References

[1] Y. Chabre, J. Pannetier, Prog. Solid State Chem. 23 (1995) 1.
[2] D. Guyomard, in: T. Osaka, M. Datta (Eds.), New Trends in Electrochemical Technology: Energy Storage Systems in Electronics, Gordon & Breach Publishers, Philadelphia, 2000, p. 253 (Chapter 9).
[3] L. Liu, X. Wang, R. Bontchev, K. Ross, A.J. Jacobson, J. Mater. Chem. 9 (1999) 1585.
[4] X. Wang, L. Liu, A.J. Jacobson, Z. Anorg. Allg. Chem. 624 (1998) 1977.
[5] L.I. Hill, R. Portal, A. Verbaere, D. Guyomard, Electrochem. Solid-State Lett. 4 (2001) A180.
[6] L.I. Hill, A. Verbaere, D. Guyomard, J. New Mater. Electrochem. Syst. 5 (2002) 129.
[7] L.I. Hill, H. Arrivé, D. Guyomard, Ionics 8 (2002) 161.
[8] L.I. Hill, A. Verbaere, D. Guyomard, J. Electrochem. Soc. 150 (2003) D135.
[9] L.I. Hill, A. Verbaere, D. Guyomard, J. Power Sources 119–121 (2003) 226.
[10] A.D. Roberston, A.R. Armstrong, P.G. Bruce, Chem. Mater. 13 (2001) 2380.
[11] L. Sanchez, J. Farcy, J.-P. Pereira-Ramos, L. Hernan, J. Morales, J.L. Tirado, J. Mater. Chem. 6 (1996) 37.
[12] S. Franger, S. Bach, J. Farcy, J.P. Pereira-Ramos, N. Baffier, J. Power Sources 109 (2002) 262.
[13] S. Sarciaux, A. Le Gal La Salle, A. Verbaere, Y. Piffard, D. Guyomard, Mater. Res. Soc. Symp. Proc. 548 (1999) 251.
[14] P.M. De Wolff, Acta Crystallogr. 12 (1959) 341.
[15] E. Machefaux, L.I. Hill, A. Verbaere, D. Guyomard, Chem. Mater., submitted for publication.
[16] S. Sarciaux, A. Le Gal La Salle, A. Verbaere, Y. Piffard, D. Guyomard, J. Power Sources 81–82 (1999) 656.
[17] S. Sarciaux, A. Le Gal La Salle, A. Verbaere, Y. Piffard, D. Guyomard, J. Power Sources 81–82 (1999) 661.